Trimerization of Monocyanate Ester in Nanopores

Yung P. Koh and Sindee L. Simon*

Department of Chemical Engineering, Texas Tech University, Lubbock, Texas 79409

Received: December 29, 2009; Revised Manuscript Received: February 27, 2010

The effects of nanoconfinement on the reaction kinetics and properties of a monocyanate ester and the resulting cyanurate trimer are studied using differential scanning calorimetry (DSC). On the basis of both dynamic heating scans and isothermal reaction studies, the reaction rate is found to increase with decreasing nanopore size without a change in reaction mechanism. Both the monocyanate ester reactant and cyanurate product show reduced glass transition temperatures (T_gs) as compared to the bulk; the T_g depression increases with conversion and is more pronounced for the fully reacted product, suggesting that molecular stiffness influences the magnitude of nanoconfinement effects. Our results are consistent with the accelerated reaction and the T_g depression found previously for the nanoconfined difunctional cyanate ester, supporting the supposition that intracyclization is not the origin of these effects.

Introduction

The properties of materials confined to the nanoscale dimensions differ from the bulk, depending on the confinement system, material studied, and the measurement technique.[1−3] Among the properties examined in nanoconfinement studies, many have focused on the changes in the glass transition temperature (T_g), since the glass temperature is one of the most important properties of a material, dictating, for example, application temperature range. It is generally accepted that the glass transition temperature at the nanoscale is depressed relative to the bulk unless strong interactions between the confined material and the confinement medium are present. Potential explanations include intrinsic size effects[1−6] and enhanced mobility at the surface[7−13] coupled with a larger surface-to-volume ratio with decreasing confinement size; however, more systematic studies are still required to explain the large range of seemingly contradictory results in the literature.

Nanoconfinement not only results in a change in T_g and associated dynamics, but it can also result in changes in reactivity. Recently, Huck[14] showed the possibility of using nanoconfinement as a synthetic tool to obtain desirable reactivity, selectivity, or yield through modification of the local chemical and conformational environment. Indeed, self-assembled monolayers, in which molecules are confined to a monolayer on surfaces, showed 3 orders of magnitude slower reaction rate than that of bulk reaction of alkaline hydrolysis of *N*-hydroxysuccinide ester due to steric crowding at the surface.[15] On the other hand, nanoscale energetic materials, such as thermites, lead to faster burning rates relative to the bulk and, thus, improved performance. The enhanced reactivity of nanoscale thermites is presumably due to enhanced heat and mass transfer by the proximity of molecules and larger interfacial area at the nanoscale.[16,17]

Recently, Li and Simon[18,19] found that nanopore confinement increased the reaction rate of bisphenol M dicyanate ester by a factor of 20 in 11.5 nm hydrophobic pores without a change in the kinetic rate law. In this reaction, three cyanate ester functional groups react to form a triazine ring, and since the reactant is difunctional, a three-dimensional thermosetting network structure results. However, a monomer intracyclization side reaction can occur in this system,[20,21] and if it occurred with greater probability under nanoconfinement, the side reaction could lead to both the enhanced reactivity and depressed T_g observed relative to the unconfined bulk reaction.[19] It was argued that the probability of monomer intracyclization did not change, as evidenced by the fact that the T_g versus conversion relationship and the gel point did not change under nanoconfinement.[18,19] To further corroborate this conclusion, here we examine reaction of a monofunctional cyanate ester under nanoconfinement, since the monofunctional nature of the reactant precludes monomer intracyclization. Hence, the purpose of this study is to investigate the effects of nanoconfinement on the reaction kinetics and glass transition temperature of monofunctional cyanate confined in the nanopores of controlled pore glasses. In particular, we examine the behavior in silanized hydrophobic nanopores in this work and compare the results to those found for difunctional cyanate ester under the same confinement.

Methodology

Materials. The monofunctional cyanate ester used in this study is 4-cumylphenol cyanate ester, obtained from Oakwood Products and used as received. Its molecular weight is 237.3 g/mol. Three 4-cumylphenol cyanate esters react by trimerization of the three OCN groups to form a cyanurate trimer with molecular weight of 711.9 g/mol. The chemical structure of the monofunctional cyanate ester reactant and the resulting trimerization product are shown in Figure 1.

Controlled pore glass (CPG), produced by Millipore, is used as a nanoconfinement matrix. Four different pore sizes of CPGs are employed, ranging from 8.1 to 122.1 nm. The detailed specifications of each CPG are listed in Table 1, as provided by the manufacturer. The native CPG is made from borosilicate glass and inherently contains hydroxyl groups on its surface. Cleaning with nitric acid was followed by a silanization treatment to replace the hydrophilic hydroxyl groups with hydrophobic trimethylsilyl groups following the procedure of Jackson and McKenna[22] using hexamethyldisilazane (Sigma-Aldrich). The silanization treatment has been reported to result

* Corresponding author. E-mail: sindee.simon@ttu.edu.

10.1021/jp912235c
Published on Web 05/24/2010

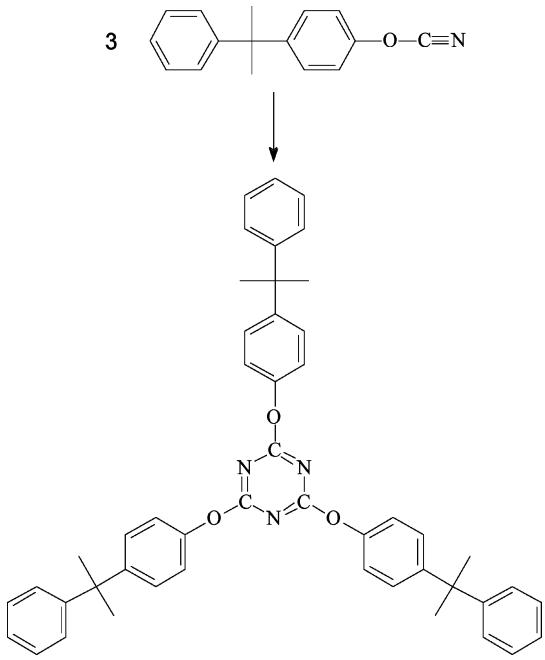

Figure 1. The trimerization reaction of 4-cumylphenol cyanate ester to produce its cyanurate product.

TABLE 1: Specifications of Controlled Pore Glasses

product name	mean pore diameter (nm)[a]	pore diameter distribution (%)[b]	specific pore volume (cm^3/g)[a]	specific surface area (m^2/g)[c]
CPG00080	8.1	9.0	0.49	197.0
CPG00130	13.0	7.4	0.68	130.0
CPG00500	50.0	3.7	1.10	50.9
CPG01200	122.1	3.7	1.73	31.2

[a] Determined by mercury intrusion method. [b] Analyzed by ultrasonic sieving method. [c] Measured by nitrogen adsorption method.

in negligible changes in pore diameter and pore size distribution.[23] The silanized CPGs were stored in a desiccator before use.

The borosilicate CPG is expected to be insoluble in the monocyanate ester and the resulting cyanurate product. Backing up this assertion that organic liquids do not leach material out of the CPG, the melting point depression of benzene in 8.1 nm CPG nanopores, silanized with hexamethyldisilazane, was measured 10 min after initial imbibement and as a function of time after imbibement for times up to 1 week. The melting point depression, measured in slightly overfilled pores by the difference in the onset of melting between benzene in the pores and the bulk material external to the pores, was found to be constant at 16.10 ± 0.03 K in 8.1 nm pores for times from 10 min up to 1 week. The results indicate that the CPG nanopores are a stable matrix for nanoconfinement of organic liquids.

In addition to the preparation and reaction of the monocyanate ester samples in all of the sizes of nanopores, we also reacted monocyanate ester in the bulk unconfined state and then imbibed the cyanurate product in 13 nm pores to examine whether the T_g depression depended on reaction conditions. The imbibement of the cyanurate was monitored for two weeks at 160 °C by measuring T_g as a function of imbibement time; complete imbibement was accomplished in 1 week. As shown later, the T_g depression is the same within the error of the measurements for the nanoconfined cyanurate, regardless of whether it was synthesized in the pores or synthesized in the bulk and then imbibed in the pores.

DSC Measurements. A Perkin-Elmer Pyris 1 differential scanning calorimeter (DSC) was used with an intracooler maintained at −80 °C for T_g measurements when T_g was above −30 °C; a liquid nitrogen cooling system maintained at −150 °C was used when T_g was below −30 °C. For the intracooler system, measurements were made in a nitrogen atmosphere, whereas for the liquid nitrogen system, a helium atmosphere was employed due to helium's better thermal conductivity at low temperatures.

Samples were prepared by first putting ∼2−6 mg of CPG in a hermetic DSC pan, followed by placing monocyanate ester on top of the CPG. The CPGs are all underfilled, and the pore fullness ranges from 70% to 90%, as calculated from pore volume and monocyanate ester loading volume, the latter of which ranged from 2 to 4 mg. We found that the T_g and heat of reaction were independent of both the degree of pore fullness and the sample size; similar results have been reported for a dicyanate ester in silanized pores[18] and for T_g of hydrogen-bonding liquids in silanized pores.[24] All samples were prepared under a nitrogen blanket to minimize adsorption of adventitious water. Although the monocyanate ester is a liquid at ambient conditions and is imbibed into the CPG in a few minutes by capillary forces,[22] to ensure the complete imbibement, we waited at least 2 h between sample preparation and DSC measurement. A similar procedure was used to imbibe the fully reacted trimer into 13 nm pores, except imbibement was accomplished at 160 °C for two weeks, as already mentioned.

The effects of nanoconfinement on the reactivity and properties were examined by measuring the limiting fictive temperature (T_f') and the residual heat of reaction after isothermal reaction for times ranging from 0 to 4.2 days at 141 °C. As the reaction proceeds, the fictive temperature increases from that of reactant to that of the product, and the residual heat of reaction decreases from the total heat of reaction to zero residual heat at the end of reaction. The limiting fictive temperature is determined at 10 K/min after cooling at 30 K/min from the intersection of the extrapolated liquid and glass enthalpy lines obtained from integration of the heat flow following the method of Moynihan et al.[25] Although the glass transition temperature is correctly measured only on cooling from the equilibrium state,[26] its value at a given rate (β) can be approximated by the limiting fictive temperature measured on heating after cooling at the same rate β.[26−28] Hence, we refer to T_f' equivalently as T_g in this study. The residual heat of reaction is used to calculate the conversion as a function of reaction time:

$$x = \frac{\Delta H_T - \Delta H_r}{\Delta H_T} \quad (1)$$

where ΔH_T is the total heat of reaction of an initially unreacted monocyanate ester and ΔH_r is the residual heat for a partially reacted sample at a given reaction time.

Two types of experiments were performed. In the first, termed method 1, an initially unreacted sample was scanned to 141 °C, partially reacted at 141 °C for a prespecified time, cooled, and then rescanned to 141 °C to obtain T_g for the given reaction time. Further reaction at 141 °C was then accomplished, followed by cooling and rescanning to 141 °C to obtain T_g at a longer reaction time. This cycle was continued until complete reaction was reached. In this way, one sample was used to obtain T_g versus reaction time data, reducing errors associated with multiple samples. The reaction temperature of 141 °C was chosen such that the trimerization reaction of the bulk was not

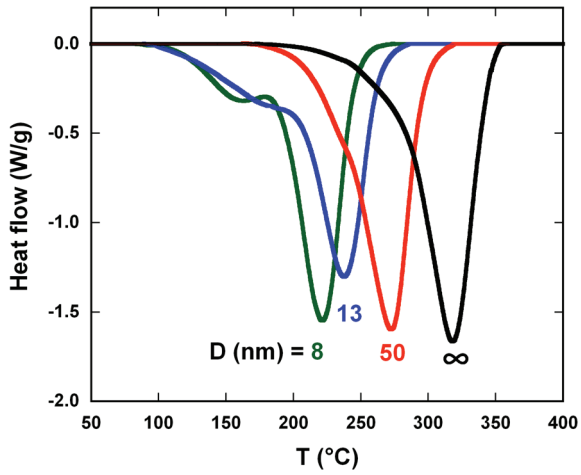

Figure 2. DSC heating scans of initially unreacted monocyanate ester at 10 K/min heating rate for the bulk and samples in nanopores of diameter D as indicated.

too slow (i.e., the reaction was completed within 5 days), while at the same time, the reaction under the smallest nanopore constraint was not too fast (i.e., the reaction took a minimum of several hours). In the second type of experiment, termed method 2, both T_g and the residual heat of reaction were obtained after reaction for reaction times ranging from 0 to 4.2 days. This second experiment, in which a different sample was used for each reaction time, provided the relationship between T_g and conversion x, as well as a serving as a check on our primary methodology.

The DSC temperature was calibrated with *n*-octane, gallium, and indium at 10 K/min on heating. The isothermal calibration, which is relevant for the isothermal reaction temperature, was performed at 0.1 K/min, which was found in other work[29] to be equivalent to performing an isothermal calibration. The heat flow of the DSC was calibrated with indium. Separate calibrations were performed for two types of cooling systems used.

Results

Dynamic Scans of Initially Unreacted Monocyanate Ester. The reaction exotherms of initially unreacted monocyanate ester in both bulk and nanoconfined states are shown in Figure 2. The DSC heating scans were performed at the heating rate of 10 K/min. As the nanopore size decreases, the exotherm moves to lower temperatures, indicating that the trimerization of monocyanate ester is accelerated with decreasing nanopore size. The reaction onset temperature, determined by the intersection of the baseline with a line drawn tangent to the steepest part of the primary exotherm on the low-temperature side, is a measure of reactivity and shifts to lower temperatures under nanoconfinement. Although the reaction rate is enhanced at the nanoscale, the total exotherm area or heat of reaction (per mol reactant) is the same for the bulk and nanoconfined samples, within the measurement error of 1.3% for the bulk and as high as 3.9% for the nanoconfined samples, indicating that the overall reaction mechanism is unchanged and that the reaction goes to completion at the nanoscale. Both the reaction onset temperature and the total heat of reaction as a function of nanopore size are tabulated in Table 2. The reaction onset temperatures for the bulk and nanoconfined difunctional cyanate ester polycyanurate system similarly decrease with decreasing nanopore size, and the heat of reaction for the difunctional system is similarly independent of confinement size, with a value of 111.6 ± 4.3 J/mol OCN,[18] similar to that measured here.

TABLE 2: Total Heat of Reaction and Onset Temperature of the Reactant under Nanoscale Constraints at Different Sizes

	D (nm)				
	∞	122.1	50.0	13.0	8.1
ΔH (kJ/mol)	104.1 ± 1.3	105.0 ± 3.1	104.1 ± 5.4	103.4 ± 4.1	102.5 ± 3.5
T_{onset} (°C)	277.4 ± 6.6	235.4 ± 3.4	232.6 ± 1.2	202.6 ± 3.1	192.3 ± 1.3

The low-temperature shoulder of the exotherm in Figure 2 becomes more pronounced as nanopore size decreases, and for material confined to 8 nm pores, the shoulder is quite distinct. Because the adsorption of water can also result in the shoulder of the exotherm,[30,31] the heating rate dependence of the shape of the exotherm was examined in Figure 3 for the bulk and nanoconfined sample in 13 nm CPG. The low-temperature shoulder of the exotherm appears as the heating rate decreases not only for the 13 nm CPG confined sample but also for the bulk. Since care was taken to prepare all samples under a nitrogen blanket to avoid adventitious water and since there is no expectation of adventitious water in the bulk samples, the shoulder of the exotherm in Figure 2 is suggested to reflect the complex trimerization reaction mechanism, which involves multiple steps. However, although the shape of the exotherm is a function of the scan rate, the heats of reactions are independent of the heating rate within experimental error. Also shown in Figure 3, the activation energy calculated from the shift in the exotherms with heating rate using the isoconversion method[32]

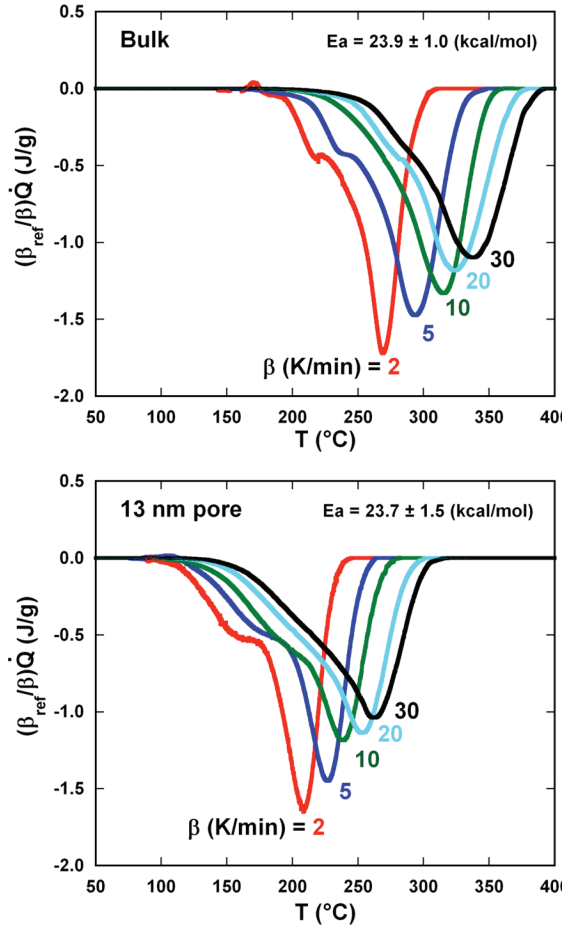

Figure 3. DSC heating scans of initially unreacted monocyanate ester at different heating rates, β, for the bulk and samples in 13 nm nanopores. The heat flow (y axis) is scaled by β_{ref}/β, where β_{ref} is 10 K/min.

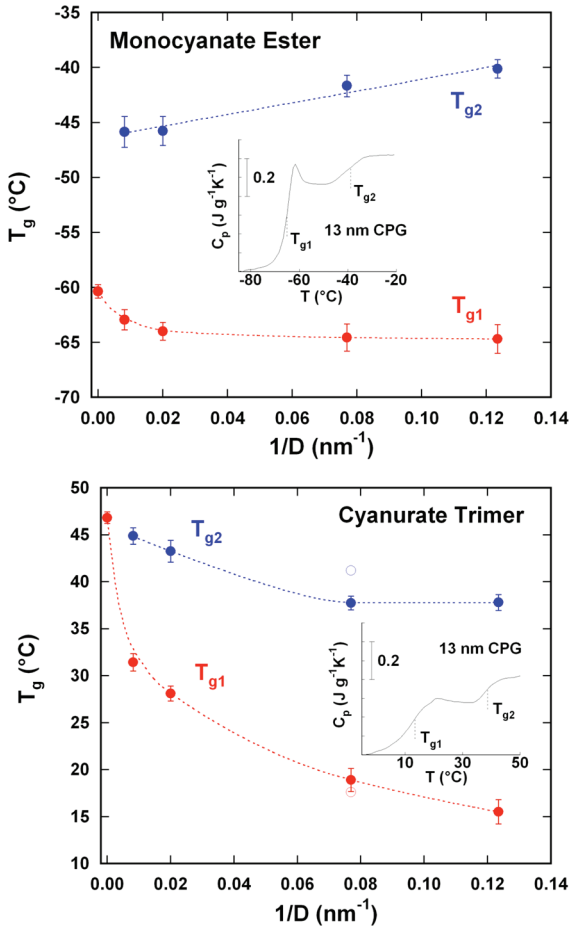

Figure 4. Glass transition temperature of monocyanate ester reactant (upper figure) and for the cyanurate trimer (lower figure) as a function of reciprocal pore diameter, D. The open symbols are the cyanurate trimer reacted in the bulk unconfined state and then imbibed in 13 nm nanopores. Typical DSC traces showing the two T_gs are shown in the insets.

is unchanged at the nanoscale, being 23.7 ± 1.5 kcal/mol at 13 nm and 23.9 ± 1.0 kcal/mol for the bulk reaction.

T_g Depression of Unreacted Monocyanate Ester and Cyanurate Trimer. The T_g of unconfined or bulk monocyanate ester is −60.3 ± 0.6 °C, and upon reaction, the value increases to that of the fully reacted cyanurate product at 46.8 ± 0.6 °C, a 100 K increase over that of the monocyanate ester. As expected, the T_gs of nanoconfined monocyanate ester reactant and the fully reacted cyanurate product are depressed relative to the bulk, as shown in Figure 4a and b, respectively, as a function of reciprocal nanopore size. Two T_gs are observed for both reactant and product confined in all nanopores, and these are designated T_{g1} and T_{g2}, respectively; typical scans showing the two T_gs in 13 nm pores are shown in the insets of the figures. For the monocyanate ester reactant, the primary T_g (T_{g1}) decreases slightly with decreasing nanopore size and is depressed by 4.3 ± 1.3 K at 8.1 nm confinement, whereas the secondary T_g (T_{g2}) is 18−25 K above T_{g1}, increasing slightly with decreasing nanopore size, and always higher than the bulk unconfined T_g. On the other hand, for the cyanurate product, T_{g1} decreases significantly with decreasing nanopore size and is depressed by 31.3 ± 0.9 K in 8.1 nm pores, whereas T_{g2} is 15−30 K above T_{g1} and decreases slightly with decreasing pore size. Interestingly, T_{g2} of the nanoconfined cyanurate product is lower than the T_g of the bulk cyanurate.

Shown also in Figure 4b, open symbols are the glass transition temperatures of the cyanurate trimer reacted in the bulk unconfined state and then imbibed in 13 nm nanopores. The value of T_{g1} is 17.6 °C and the value of T_{g2} is 41.2 °C, within 2 and 4 °C, respectively, of the values obtained for the material synthesized in the 13 nm nanopores. Hence, the depression in T_g and the presence of T_{g2} is not influenced by reaction under nanoconfinement, but rather appears to be a result of the confinement of the glass-former itself.

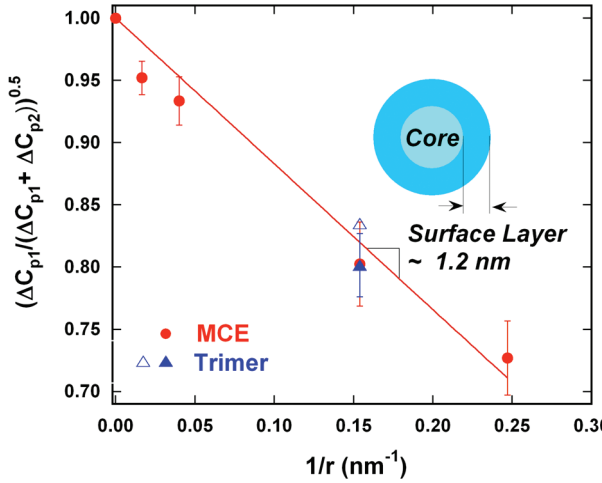

Figure 5. Square root of the fractional heat capacity change at T_{g1} vs reciprocal pore radius. The open symbol is the cyanurate trimer reacted in the bulk unconfined state and then imbibed in 13 nm nanopores. Assuming the two-layer model of core plus surface layer, shown schematically, the thickness of the latter is obtained from the slope.

Two T_gs at the nanoscale are commonly reported in the literature,[18,19,22,33−38] and the origin has been explained using a two-layer model,[33] consisting of a more mobile core and less mobile surface layer. The decreased mobility of the surface layer can be attributed to physical (mechanical interlocking) or chemical interactions, or both, between the nanoconfined material and nanoconfining medium. The length scale of the surface layer can be determined assuming that the volume of material in a given layer is proportional to the step change of the heat capacity for that layer, that the density of the material does not change along the pore radius, and that the shape of pore is cylindrical:[38]

$$\frac{\Delta C_{p2}}{\Delta C_{p1}} = \frac{V_s}{V_c} = \frac{r^2 - (r-d)^2}{(r-d)^2} \qquad (2)$$

where ΔC_{p2} is the step change of heat capacity at T_{g2}, ΔC_{p1} is the step change of heat capacity at T_{g1}, V_s is the volume of material in the surface layer, V_c is the volume of material in the core, r is the nanopore radius, and d is the surface layer thickness. By rearranging eq 2, we obtain eq 3, which is used in the calculation of the surface layer, d.

$$\sqrt{\frac{\Delta C_{p1}}{\Delta C_{p1} + \Delta C_{p2}}} = 1 - \frac{d}{r} \qquad (3)$$

Hence, the surface layer thickness can be determined from the slope of a plot of the square root of the fractional step change of the heat capacity at T_{g1} versus the reciprocal pore radius; the result is shown in Figure 5 for unreacted monocyanate ester and fully reacted cyanurate. The resulting thickness of the surface layer is 1.2 nm with a standard error of fit of 0.1 nm, which is consistent with the cooperative length scale associated

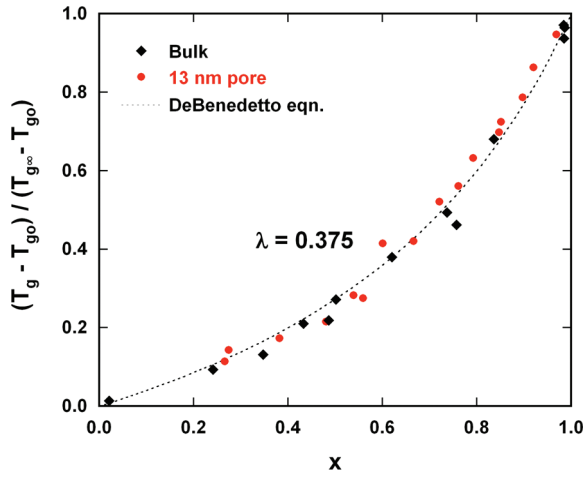

Figure 6. Dimensionless T_g as a function of conversion of monocyanate ester reacted in the bulk and in 13 nm nanopores. The solid line is the best fit to the Debenedetto equation with the fitting parameter λ value of 0.375.

with T_g.[39] The thickness of the surface layer for our nanoconfined monofunctional cyanate ester and its cyanurate product in controlled pore glass (CPG) is also comparable to that of difunctional cyanate ester in silanized and native CPG (d = 0.9 nm)[18,19] as well as to polystyrene/*o*-TP (*o*-terphenyl) in CPG (d = 1.0−2.5 nm)[38] and glycerol in CPG (d = 0.9 nm),[24] although it differs from that for propylene glycol in Gelsil nanopores (d = 0.15 nm).[40]

Isothermal Reaction Kinetics. The glass transition temperature is employed as a kinetic parameter to monitor the progress of reaction as a function of reaction time in this study. Following T_g is akin to following conversion, since T_g and conversion have a unique one-to-one relationship[18,41] given by the DeBenedetto equation,[42]

$$T_g^* = \frac{T_g - T_{g0}}{T_{g\infty} - T_{g0}} = \frac{\lambda x}{1 - (1 - \lambda)x} \tag{4}$$

where λ is a structure-dependent parameter, T_g^* is the dimensionless glass transition temperature, T_{g0} is the T_g of the unreacted monocyanate ester, and $T_{g\infty}$ is the T_g of the completely reacted cyanurate trimer. The advantage of using T_g instead of conversion to follow the reaction is that T_g is sensitive and is easily and accurately determined.[43] The error in the T_g measurement is ∼1 K, and the change in T_g with conversion is 105 K (for the bulk), giving an error of ∼1.0%; on the other hand, the error in the heat of reaction is 1.3−3.9% initially, depending on pore size, and increases as the residual heat decreases. In addition, only one sample is needed to obtain the entire T_g versus reaction time data (using the experimental procedure method 1 described earlier), whereas each conversion data point consumes one sample, since after the residual heat of reaction is measured, the sample is fully reacted.

Figure 6 shows the relationship between T_g and conversion for the bulk unconfined sample and for the sample confined in 13 nm pores. The relationship is unchanged by the nanopore confinement, similar to our prior results for a difunctional cyanate ester.[18] It must be noted that since two T_gs exist at the nanoscale, the T_g value of the 13 nm nanopore is the average glass transition temperature determined on the basis of the primary and secondary T_g values, weighted by their corresponding heat capacity changes at T_g:[18]

$$T_{g,avg} = \frac{T_{g1}\Delta C_{p1} + T_{g2}\Delta C_{p2}}{\Delta C_{p1} + \Delta C_{p2}} \tag{5}$$

The dotted line in Figure 6 is the best fit to the DeBenedetto equation using λ as a fitting parameter, and the resulting value of λ is 0.375 with a standard error of 0.012. A derivation of the DeBenedetto equation,[44] in which it is assumed that T_g is an isentropic transition and that the mixture of the initial reactant and final product is an ideal solution, relates λ to the step changes in the heat capacities of the reactant and product, ΔC_{po} and $\Delta C_{p\infty}$, respectively:[44]

$$\lambda = \frac{\Delta C_{p\infty}}{\Delta C_{po}} \tag{6}$$

It is noted that the DeBenedetto equation reverts to the Gordon−Taylor equation for a binary mixture (as we have here), and the same theoretical parameter is expected.[45,46] The experimental value of $\Delta C_{p\infty}/\Delta C_{po}$ is 0.401/0.562 = 0.712 ± 0.016 for our system, much different from the fitted value of λ = 0.375 ± 0.012. The inconsistency between theoretical and experimental values is a result of the ideal mixing assumption in the theoretical derivation. Indeed, the bulk cyanurate trimer can crystallize during the reaction and shows a broad melting transition with an onset ranging from 115 to 130 °C (decreasing with increasing crystallinity), indicating phase separation of the cyanurate and monocyanate ester, that is, nonideal solution behavior. Consequently, the fitting parameter λ is not equal to the theoretical value. Despite this, the DeBenedetto equation still describes the experimental data very well, as shown in Figure 6.

The evolution of the primary T_{g1} and secondary T_{g2} as a function of reaction time at the isothermal temperature of 141 °C is shown in Figure 7a and b, respectively. T_g increases from the T_g of the initially unreacted monocyanate ester (T_{g0}) as the reaction proceeds, and then T_g levels off at full conversion and has a final value corresponding to that of the cyanurate trimer product ($T_{g\infty}$), the value of which decreases with decreasing pore size, as already discussed in Figure 4. The consistency between the two methodologies used to obtain data (single sample versus multiple samples) is demonstrated by the solid and open symbols for 13 nm and bulk data. In addition, the reproducibility of the method 1 (single sample) results is demonstrated by the agreement of the solid symbols and the + and × symbols for the bulk data.

Perhaps more important than the effect of nanoconfinement on $T_{g\infty}$, the T_g-versus-reaction time curves shift to shorter time with decreasing nanopore size. Hence, the trimerization reaction is accelerated as pore size decreases, consistent with the shift of the exotherms to lower temperatures in the dynamic scans, as shown in Figure 2. The bulk reaction kinetics of monofunctional cyanate ester follow a first-order plus first-order autocatalytic reaction model,

$$\frac{dx}{dt} = k(1 - x)(x + b) \tag{7}$$

where x is conversion, t is reaction time, and k is the Arrhenius rate constant for the first-order autocatalytic reaction. The constant b has been related to the fraction of trace impurities which catalyze the reaction initially.[41] In addition, any differences in the activation energies of the first order and first-order

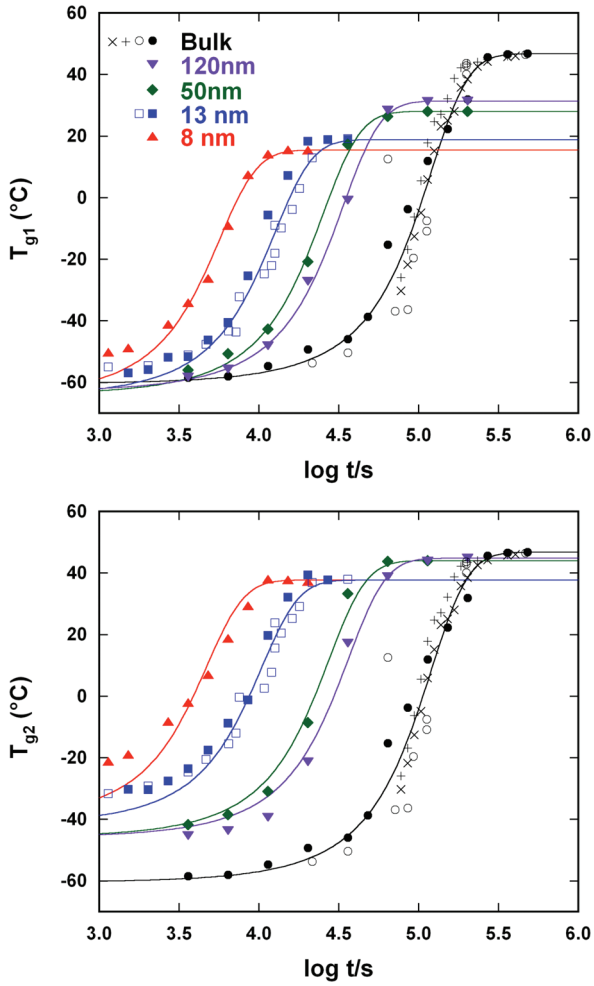

Figure 7. Glass transition temperature as a function of logarithmic reaction time in the bulk and for material confined in nanopores for T_{g1} (upper figure) and T_{g2} (lower figure) at the reaction temperature of 141 °C. Solid symbols and + and × symbols represent the data obtained by method 1 (single sample). Open symbols represent the data obtained by method 2 (multiple samples). The solid lines are the best fit to the reaction model. Only one T_g is observed for the bulk, and these values are plotted in both figures.

autocatlytic reactions are also incorporated into *b*. Coupling the kinetic rate equation with the DeBenedetto equation (eq 4) yields T_g as a function of reaction time. The solid lines shown in Figure 7 are the best fits to both the bulk and nanoconfined experimental data. It is clear that the reaction model describes the experimental results well for both the bulk and nanoconfined samples, indicating the reaction model and overall reaction mechanism are unchanged at the nanoscale, consistent with the unchanged heat of reaction and unchanged activation energy, and similar to prior results for a dicyanate ester reaction.[18]

The magnitude of the reaction acceleration can be quantified by the acceleration factor, α:

$$\alpha = \frac{k}{k_{bulk}} \tag{8}$$

where *k* is the rate constant obtained by fitting eq 7 to the data and k_{bulk} is the rate constant for the bulk unconfined sample. The α value for the bulk sample is 1.0 by definition. Figure 8 shows the resulting acceleration factor as a function of reciprocal nanopore size. The acceleration factor of monocyanate ester is

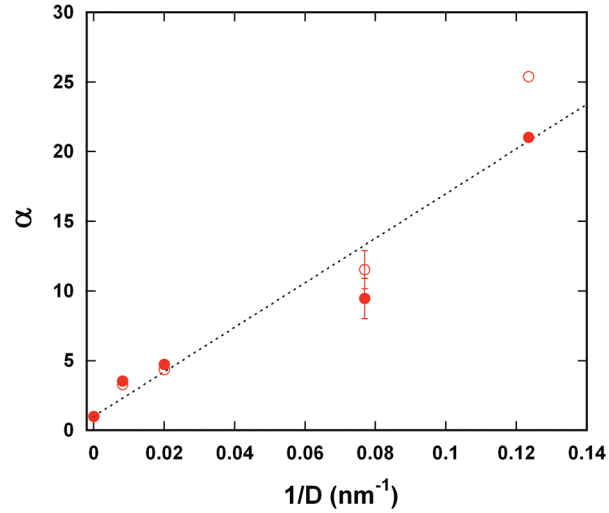

Figure 8. The acceleration factor as a function of reciprocal pore diameter for T_{g1} (solid symbols) and for T_{g2} (open symbols). The dashed line is intended only as a guide to the eye.

similar for the primary T_{g1} and secondary T_{g2} data. The acceleration factor increases with decreasing nanopore size, with the reaction rate being accelerated by a factor of 21 in 8 nm pores (as measured by T_{g1}).

Discussion

In this study, nanoconfinement accelerates the trimerization reaction relative to the bulk. The enhanced reactivity at the nanoscale has been suggested to be due to an enhanced collision efficiency or frequency induced by the presence of the nanopore surface,[18] since the proximity of the surface results in a decreased rate of reactants diffusing apart. Other explanations for the origin of the acceleration include a change in reaction mechanism at the nanoscale, the catalytic effect of the nanopore surface, or both. However, the same heat of reaction and the same kinetic rate expression for the bulk and the nanoconfined materials provide evidence that the reaction mechanism is unchanged at the nanoscale. In addition, the catalytic effect of the nanopore surface is not considered to be the cause of the enhanced reactivity on the basis of the same activation energy for the bulk and nanoconfined samples and similar acceleration factors for T_{g1} and T_{g2}. Hence, an intrinsic size effect[18] is suggested to be the reason for the enhanced reactivity under nanoconfinement. In addition, our result of the enhanced reactivity for the trimerization of monofunctional cyanate ester gives proof that the enhanced reactivity of difunctional cyanate ester under nanoconfinement[18,19] is not due to its intracyclization side reaction, since our reactant cannot cyclize due to its monofunctional nature.

The magnitude of the effects of nanoconfinement on the T_g depression is, as mentioned in the Introduction, related to the material, confinement method, and measurement technique. It has recently been suggested that the effects of nanoconfinement on T_g can be altered by modification of the molecular structure[47] or addition of diluent,[48,49] presumably through the changes in chain stiffness or in the size of the cooperatively rearranging region. Backing up the hypothesis that the magnitude of the T_g change at fixed confinement size increases with chain stiffness, we found in previous work[18,19,50] that the T_g depression in a dicyanate ester/polycyanurate material increases with increasing conversion and, thus, with increasing T_g and increasing chain stiffness. In this study, we also observe that the T_g depression

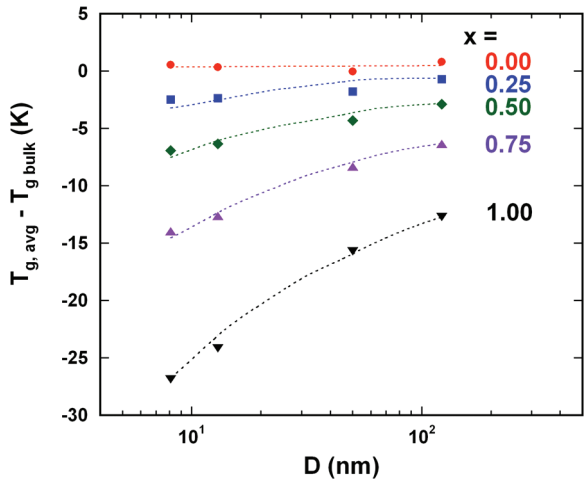

Figure 9. Change in the average glass temperature from the bulk as a function of pore diameter at different conversions, x. The dashed lines are intended only as guides to the eye.

increases with increasing conversion. This is clearly shown in Figure 9 by replotting the T_g depression of Figure 7 as a function of pore diameter for different conversions, x. In Figure 9, the average T_g was used as defined in eq 5. The change T_g in average for the unreacted monomer ($x = 0$) for a given pore size is only 1 K, but as the reaction proceeds, the magnitude of the T_g change increases with increasing conversion; that is, the degree of nanoconfinement on T_g is enhanced by the reaction. The result suggests that molecular stiffness (molecular, in this case, since our molecules are not chains) influences the magnitude of nanoconfinement effects.

There has been considerable discussion of the origin of the T_g depression in nanoconfined materials.[1−13,51−53] A leading hypothesis, particularly for researchers involved in work on polymer ultrathin films, is that higher mobility at the free surface is responsible (or partially responsible) for the T_g depression.[7−13] On the other hand, for the fully reacted cyanurate studied here, we observed a T_g depression for both T_{g1} and T_{g2}, with a larger depression always observed for T_{g1}. If the two-layer model[18,33] is correct, and we note in this regard that it is consistent with the ΔC_p data as shown in Figure 5, the fact that $T_{g1} > T_{g2}$ indicates the surface is less mobile than the core. Hence, the T_g depression in our nanoconfined system cannot readily be attributed to a greater mobility at the interface.

The value of T_{g2}, which is suggested to reflect the mobility of the surface layer, is lower than the bulk T_g for the trimer, but it is higher for MCE. We showed in previous work[19] that T_{g2} was not sensitive to surface chemistry, indicating that physical or mechanical interlocking effects dominate. Complicating the issue may be the fact that large T_g gradients cannot be supported in ultrathin layers, as shown by Ellison and Torkelson.[12] Perhaps for this reason, the value of T_{g2} seems to be directly related to the value of T_{g1} rather than related to the bulk T_g. The difference $T_{g2} - T_{g1}$ found for this cyanate ester/trimer system is 15−30 K, increasing with decreasing nanopore size; the value is in good agreement with that found for the dicyanate ester/polycyanurate system studied earlier,[50] and it is of similar magnitude to that observed by Park and McKenna for *o*-TP in silanized CPG, which shows a $T_{g2} - T_{g1}$ of ∼38 K.[38]

Conclusion

The reaction of monofunctional cyanate ester to form a cyanurate trimer is performed under the nanoconfinement of controlled pore glass nanopores. Changes in reaction rate and the glass temperature are investigated as a function of pore size using DSC. From dynamic temperature scans, the trimerization reaction rate is found to be shifted to lower temperatures as pore size decreases. From isothermal reaction studies, the trimerization reaction of monocyanate ester is found to be faster as pore size decreases with an acceleration of ∼21 relative to the bulk reaction rate for cyanate ester in 8 nm pores (based on T_{g1}). Both the monocyanate ester reactant and cyanurate product show lower T_gs upon nanoconfinement, as compared to the bulk; the T_g depression increases with conversion and is more pronounced for the fully reacted product, suggesting that molecular stiffness influences the magnitude of nanoconfinement effects. The heat of reaction, activation energy, and reaction kinetic model are unchanged under nanoconfinement, suggesting that intrinsic size effects are the origin of the enhanced reactivity for the nanopore confinement. In addition, our results of monofunctional cyanate ester are consistent with the accelerated reaction and the T_g depression found previously for the nanoconfined difunctional cyanate ester, supporting the assertion that intracyclization is not the origin for these effects, since our monocyanate ester cannot intracyclize due to its monofunctional nature.

Acknowledgment. The authors gratefully acknowledge funding from the American Chemical Society Petroleum Research Fund 45416-AC7 and funding from the Texas Higher Education Coordinating Board Advanced Research Program.

References and Notes

(1) Alcoutlabi, M.; McKenna, G. B. *J. Phys.: Condens. Matter* **2005**, *17*, R461.
(2) Forrest, J. A.; Jones, R. A. L. *Polymer Surface Interfaces and Thin Films*; Karim, A., Kumar, S., Eds.; World Scientific: Singapore, 2000.
(3) Alba-Simionesco, C.; Coasne, B.; Dosseh, G.; Dudzidak, G.; Gubbins, K. E.; Randhakrishnan, R.; Sililinska-Bartkowiak, M. *J. Phys.: Condens. Matter* **2006**, *18*, R15.
(4) Alba-Simionesco, C.; Dosseh, G.; Dumont, E.; Frick, B.; Geil, B.; Morineau, D.; Teboul, V.; Xia, Y. *Eur. Phys. J. E* **2003**, *12*, 19.
(5) Morineau, D.; Xia, Y.; Alba-Simionesco, C. *J. Chem. Phys.* **2002**, *117*, 8966.
(6) McKenna, G. B. *Eur. Phys. J. E* **2003**, *12*, 191.
(7) Forrest, J. A.; Dalnoki-Veress, K. *Adv. Colloid Interface Sci.* **2004**, *94*, 167.
(8) Forrest, J. A.; Mattson, J. *J. Phys. IV* **2000**, *10*, 251.
(9) Forrest, J. A.; Dalnoki-Veress, K.; Dutcher, J. R. *Phys. Rev. E* **1997**, *56*, 5705.
(10) Dalnoki-Veress, K.; Forrest, J. A.; Murray, C.; Cigault, C.; Dutcher, J. R. *Phys. Rev. E* **2001**, *63*, 031801.
(11) Forrest, J. A.; Dalnoki-Veress, K.; Stevens, J. R.; Dutcher, J. R. *Phys. Rev. Lett.* **1996**, *77*, 2002.
(12) Ellison, C. J.; Torkelson, J. M. *Nat. Mater.* **2003**, *2*, 695.
(13) Sharp, J. S.; Forrest, J. A. *Phys. Rev. Lett.* **2003**, *91*, 235701.
(14) Huck, W. T. S. *Chem. Commun.* **2005**, 4143.
(15) Schonherr, H.; Feng, C.; Shovsky, A. *Langmuir* **2003**, *19*, 10843.
(16) Aumann, C. E.; Skofronick, G. L.; Martin, J. A. *J. Vac. Sci. Technol.* **1995**, *B13*, 1178.
(17) Kwon, Y. S.; Gromov, A. A.; Ilyin, A. P.; Popenko, E. M.; Rim, G. H. *Combust. Flame* **2003**, *133*, 385.
(18) Li, Q. X.; Simon, S. L. *Macromolecules* **2008**, *41*, 1310.
(19) Li, Q. X.; Simon, S. L. *Macromolecules* **2009**, *42*, 3573.
(20) Li, Q. X.; Simon, S. L. *Macromolecules* **2007**, *40*, 2246.
(21) Korshak, V. V.; Pankratov, V. A.; Ladovskaya, A. A.; Vinogradova, A. V. *J. Polym. Sci., Part A: Polym. Chem.* **1978**, *16*, 1697.
(22) Jackson, C. L.; McKenna, G. B. *J. Chem. Phys.* **1990**, *93*, 9002.
(23) Erb, V. Diploma Thesis, Max-Planck-Institut fur Polymerforschung, Mainz, 1993.
(24) Gorbatschow, W.; Arndt, M.; Stannarius, R.; Kremer, F. *Europhys. Lett.* **1996**, *35*, 719.
(25) Moynihan, C. T.; Macedo, P. B.; Montrose, C. J.; Gupta, P. K.; DeBolt, M. A.; Dill, J. F.; Dom, B. E.; Drake, P. W.; Easteal, A. J.; Elterman, P. B.; Moeller, R. P.; Sasabe, H.; Wilder, J. A. *Ann. NY Acad. Sci.* **1976**, *279*, 15.

(26) Badrinarayanan, P.; Zheng, W.; Li, Q. X.; Simon, S. L. *J. Non-Cryst. Solids* **2007**, *353*, 2603.
(27) Moynihan, C. T.; Easteal, A. J.; DeBolt, M. A.; Tucker, J. *J. Am. Ceram. Soc.* **1976**, *59*, 12.
(28) Plazek, D. J.; Frund, Z. N. *J. Polym. Sci., Part B: Polym. Phys.* **1990**, *28*, 431.
(29) Simon, S. L.; Sobieski, J. W.; Plazek, D. J. *Polymer* **2001**, *42*, 2555.
(30) Barton, J. M.; Hamerton, I.; Jones, J. R. *Polym. Int.* **1993**, *31*, 95.
(31) Gomez, C. M.; Recalde, I. B.; Mondragon, I. *Eur. Polym. J.* **2005**, *41*, 2734.
(32) Flynn, J. H.; Wall, L. A. *Polym. Lett.* **1966**, *4*, 323.
(33) Arndt, M.; Stannarius, R.; Gorbatschow, W.; Kremer, F. *Phys. Rev. E* **1996**, *54*, 5377.
(34) Schonhals, A.; Goering, H.; Schick, C.; Frick, B.; Zorn, R. *Colloid Polym. Sci.* **2004**, *282*, 882.
(35) Schuller, J.; Richert, R.; Fischer, E. *Phys. Rev. B* **1995**, *52*, 15232.
(36) Patkowski, A.; Ruths, T.; Fischer, E. *Phys. Rev. E* **2003**, *67*, 021501.
(37) Streck, C.; Mel'nichenko, Y. B.; Richert, R. *Phys. Rev. B* **1996**, *53*, 5341.
(38) Park, J. Y.; McKenna, G. B. *Phys. Rev. B* **2000**, *61*, 6667.
(39) Donth, E. *Relaxation and Thermodynamics in Polymers*; Akademie Verlag: Berlin, 1992.
(40) Zheng, W.; Simon, S. L. *J. Chem. Phys.* **2007**, *127*, 194501.
(41) Simon, S. L.; Gillham, J. K. *J. Appl. Polym. Sci.* **1993**, *47*, 461.
(42) Nielsen, L. E. *J. Macromol. Sci. Rev. Macromol. Chem.* **1969**, *C3*, 69.
(43) Wisanrakkit, G.; Gillham, J. K. *J. Coat. Technol.* **1990**, *62*, 35.
(44) Couchman, P. R. *Macromolecules* **1987**, *20*, 1712.
(45) Gordon, J. M.; Rouse, G. B.; Gibbs, J. H.; Risen, W. M., Jr. *J. Chem. Phys.* **1977**, *66*, 4971.
(46) Schneider, H. A. *J. Res. Natl. Inst. Stand. Technol.* **1997**, *102*, 229.
(47) Campbell, C. G.; Vogt, B. D. *Polymer* **2007**, *48*, 7169.
(48) Ellison, C. J.; Ruszkowski, R. L.; Fredin, N. J.; Torkelson, J. M. *Phys. Rev. Lett.* **2004**, *92*, 095702.
(49) Ellison, C. J.; Mundra, M. K.; Torkelson, J. M. *Macromolecules* **2005**, *38*, 1767.
(50) Koh, Y. P.; Li, Q. X.; Simon, S. L. *Thermochim. Acta* **2009**, *492*, 45.
(51) Keddie, J. L.; Jones, R. A. L. *Isr. J. Chem.* **1995**, *35*, 21.
(52) O'Connell, P. A.; McKenna, G. B. *Science* **2005**, *307*, 1760.
(53) Koh, Y. P.; McKenna, G. B.; Simon, S. L. *J. Polym. Sci., Part B: Polym. Phys.* **2006**, *44*, 3518.

JP912235C